

FUTURE GROUND MOTIONS IN MEXICO CITY

M. Ordaz^{1,2}, E. Rosenblueth^{1,3} and E. Reinoso³

ABSTRACT

Future ground motions at a soft site of the Valley of Mexico are estimated for a postulated M 8.2 earthquake with epicentral distance of 280 km. Three techniques are used: a) semiempirical estimation of Fourier acceleration spectra at a hard -reference- site plus empirical determination of site effects through empirical transfer functions; b) semiempirical computation of Fourier spectra at the reference site with theoretical calculation of site response using 1D horizontal S-wave propagation corrected to account for surface waves; c) use of an M 6.9 recording as the Green's function of the postulated event. Results of the three techniques are competing approaches, and we illustrate a rational way to combine them and obtain a single estimate that includes information from the three approaches.

INTRODUCTION

Analysis of site effects on a large valley underlain by soft clay and other lacustrine sediments is beyond the capability of present methods and computers. If one were to use finite elements, due to the extension, depth and low shear-wave velocities the Valley of Mexico, for example, would require about 3×10^9 three-dimensional elements to give accurate results for frequencies of up to 2 Hz. This would demand a speed of computation several orders of magnitude greater than those of the fastest existing equipment. There is greater hope in use of hybrid methods, or in propagation methods on Connection Machines employing cell automata [1,2], but such methods are still not sufficiently practical.

What we do have is competing approximate approaches. This paper centers on a means for combining results of such approaches. The study is principally motivated by the high probability of a severe earthquake originating in the near future in the Guerrero Gap.

Ground motions are herein characterized by response spectral accelerations, both linear and elastoplastic.

Approaches used to evaluate site effects are: a) one-dimensional analysis of horizontal shear-wave propagation; b) empirical transfer functions between a site on relatively firm ground

¹ Instituto de Ingeniería, Universidad Nacional Autónoma de México, Aparta- 70-472, Coyoacán 04510. DF, Mexico

² Centro Nacional de Prevención de Desastres, Delfín Madrigal 665, 04360, DF, Mexico.

³ Centro de Investigación Sísmica, Camino al Ajusco 203, Tlalpan 14200, DF Mexico

ground and the station of interest; and c) synthetic records using small earthquakes as Green's functions. Correlations among these approaches are taken into account.

THE VALLEY OF MEXICO

The valley measures about 30 x 70 km (Fig. 1). It is completely surrounded by mountains. A north-south section is shown in Fig. 2, and a typical log of the first 100 m in Fig. 3. Under much of the city one finds an archaeological fill, typically 1 m thick but reaching several meters in the old center of town. The most decisive formations for seismic site effects are the very deformable clays, which can reach depths exceeding 100 m and contain sand lenses and layers. Shear-wave velocities in the upper clay deposits can be as low as 50 m/sec. However, significant wave amplification is also due to the contrast between the cretaceous limestones and the overlying deposits at depths of over 3 km in some sites.

THE EARTHQUAKES

The Valley of Mexico is affected by earthquakes having different causes. Here we shall be concerned with those due to subduction of the Cocos Plate under the North American Plate. The first macroseism for which there were appropriate strong-motion instruments in the valley was the Michoacán earthquake of 85.9.19. With a magnitude of 8.1 (all magnitudes quoted in this paper are Ms) it caused the worst natural disaster in the country's history, with the major part of the damage and casualties taking place in Mexico City. It was followed 36 hours later by one with magnitude 7.7. After that, a number of small and moderate earthquakes have been recorded (Fig. 4 and Table 1) and their records analyzed.

Statistical analyses of the sizes and times of occurrence of subduction events along Mexico's Pacific Coast have led to the conclusion that a subduction earthquake with magnitude 8.1-8.3 is likely to occur in the near future, with rupture area in the Guerrero Gap (Fig. 4). More recent monitoring of Q [3] and examination of the pattern of epifoci during the last few years [4] has increased the probability to perhaps 0.5 that the event occur within the next four years. There is a probability of 17 percent that it will be followed by one with an expected magnitude of 7.6 a few hours or up to two years later. On the other hand, it is possible that instead of the great earthquake, the energy stored be released through three or so events with magnitudes close to 8.0. In this paper we examine the ground motions that could take place during an M 8.2 earthquake occurring 280 km away from Mexico City, that is, the expected event associated with the rupture of the Guerrero Gap.

GROUND MOTION PARAMETERS

Many design decisions are made on the basis of pseudo-acceleration response spectra for linear behavior with 5 percent damping. A sample of such spectra for records obtained at various sites in the Valley of Mexico is shown in Fig. 5. The elastic response spectrum is insufficient to properly describe the behavior of real structures during strong shaking. Its importance mainly lies in its

widespread use in building codes, and in that it has served as a means to empirically calibrate the design criteria, comparing observed damages during earthquakes with response spectral levels and nominal design conditions. For these reasons it is convenient to use elastic response spectra as the first way to describe ground motion.

We have also estimated ground motion in terms of elastoplastic response spectra for fixed ductility demands. These spectra are a slightly better way to characterize strong shaking for structural purposes. However, as more structures undergo intense seismic loading, it becomes clear that correlation between observed damage and elastoplastic spectral ordinates is also low. Reasons for these discrepancies probably lie in the methods used for computing member resistances. However, as it will be shown, reductions on spectral accelerations due to nonlinear structural behavior are so dramatic at the soft sites of the valley that it would be extremely conservative to ignore this nonlinear behavior. Therefore, we include also estimates of ground motion intensities in terms of elastoplastic spectra. We estimate the duration of strong shaking, as this is needed to convert Fourier amplitude spectra into response spectra through random vibration theory, to generate time histories based on Fourier amplitude spectra and because it is of interest for the design of structures whose properties degrade under successive cycles of alternating load.

TECHNIQUES USED TO PREDICT GROUND MOTION

For illustration purposes, we have concentrated on the estimation of ground motion at a particular recording station within the Valley of Mexico. Station 56, operated by Centro de Instrumentación y Registro Sísmico AC, is located in Colonia Roma (see Fig. 1), one of the most damaged areas of Mexico City during the great Michoacán earthquake. The prevailing ground period at the site is about 2.2 sec, with an average S-wave velocity of the uppermost layers of 60 m/sec and a thickness of soft clay of about 35 m. Station 56 was installed in 1987. It has recorded several small and moderate events, which have systematically shown peak accelerations among the highest of the valley. In what follows we describe the three techniques used to estimate ground motion at Station 56 during a postulated M 8.2 earthquake in the Guerrero Gap.

The estimation process pursues computing both expected response spectra and a measure of the uncertainty involved in the estimation. Sources of uncertainty considered are also described in the following paragraphs.

Technique 1

This approach consists in: a) estimating Fourier acceleration spectra (FAS) at a relatively firm site of the valley (a station within University City referred to in this paper as CU) using the semiempirical equations derived in Ref. 1, which relate FAS with magnitude and distance; b) computing the transfer function between this site and Station 56 with Haskell's method for vertical S-wave propagation, based on a simplified stratigraphic profile of the site; c) obtaining FAS at Station 56 as the product, in the frequency domain, of FAS at the firm site and the

computed transfer function; d) estimating strong-shaking duration at the site; e) based on FAS and duration at the site, calculating the first two statistical moments of elastic and inelastic response spectral ordinates.

We have regarded as uncertain the Fourier spectral ordinates at CU, the S-wave velocities of the stratigraphic profile of the site, and the duration of strong shaking. We assigned to the Fourier spectral ordinates a multidimensional lognormal distribution with vector of means given by the semiempirical equations, and matrix of covariances obtained empirically from the same data set used to derive the equations. We also assigned lognormal distributions to the S-wave velocities, considering them independent from each other. Finally, the duration was assigned a lognormal distribution with a median value of 60 sec and coefficient of variation of 0.15.

It has been shown by several authors (e.g. Campillo et al. [6], Bard et al. [6], Sánchez-Sesma et al. [7], Seed et al.[8]) that the above mentioned procedure to compute elastic response spectra usually underestimates observed motions at soft sites of the Valley of Mexico, mainly due to lateral heterogeneities and generated surface waves. Depending on the method used to evaluate the influence of surface waves, amplification factors vary. Seed et al. [9] reach the conclusion that the motions observed at a soft site (SCT) during the Michoacán earthquake are adequately described by the percentile 75 of the computed motions (in their study uncertainty lies in the incident motion); for the sizes of variances obtained in our calculations, percentile 75 corresponds approximately to an amplification factor of 1.6 at response spectra level, independent of structural period. Sánchez-Sesma et al. [7] obtained for a simplified shape of the Valley of Mexico acceleration amplifications of more than 2 for a site located at a distance from the edge of the valley similar to that of Station 56. Based on these considerations, and some observations of bore-hole recordings at Mexico City, we applied a scaling factor of 1.6 to the accelerograms computed following steps a) to e) to take into account the effect of surface waves.

The first two statistical moments of the elastic response spectral ordinates were obtained with a perturbation technique and random vibration theory. Inelastic spectral moments, as well as crossed elastic moments, were obtained by simulating time histories based on the random FAS at the site and then computing individual inelastic response spectra. To simulate time histories based on FAS and duration we used the approach proposed by Boore [3]; five samples of the synthetic accelerograms are depicted in Fig. 6. Fig. 7 shows response spectra associated with percentiles 16, 50 and 84 obtained with this technique. Note the large reductions of spectral accelerations for ductility demands, μ , as low as 1.5.

Technique 2

The second technique is similar to the first one, except that the site response -the transfer function between CU and Station 56- has been described using empirical transfer functions obtained from small and moderate events recorded at both CU and Station 56. Ordinates of the transfer function are regarded as lognormally distributed random variables, with vector of means and matrix of covariances obtained from the data. Except for the explicit inclusion of

uncertainties, this approach has previously been used to successfully predict the elastic response spectra in the Valley of Mexico during the earthquake of 85.9.19 [11]. A sample of the time histories obtained is shown in Fig. 8, whereas Fig. 9 depicts the response spectra corresponding to the 16, 50 and 84 percentiles computed with this approach. Note that with the use of empirical transfer functions there is no need to correct for surface waves, since the spectral ratios contain all the information about soil amplification.

Technique 3

This approach consists in using the accelerogram recorded at station 56 (NS component) during the M 6.9 event of 89.4.25 (see Table 1) as an empirical Green's function of the postulated M 8.2 event. The focal distance and path to the Valley of Mexico of both the Green's function and the postulated earthquake are similar. To sum the Green's functions we used the method proposed by Joyner and Boore [12], which essentially consists in adding N subevent records with uniformly distributed random delays between 0 and the duration of the rupture. A subevent recording is obtained by scaling the observed accelerogram of the smaller earthquake; the scaling factor and number of subevents are chosen such that both the high-frequency and the low-frequency levels scale as Brune's ω^2 model [13]. In our case we fixed for the ω model a stress drop of 100 bars and used Brune's formula to compute the rupture duration of a M 8.2 event, which turned out to be 40 sec.

We present a sample of the synthetic accelerograms in Fig. 10, and in Fig. 11 we show the response spectra obtained for 16, 50 and 84 percentile levels. The only uncertainty considered comes from the randomness of the oversimplified rupture process. Both linear and nonlinear response spectral statistical moments were computed through simulations.

Discussion of results using the three techniques

We obtained expected response spectra and measures of the uncertainty in spectral ordinates from three different approaches. Results are correlated since each technique uses pieces of information also used by the others. We have assumed that there is no model uncertainty, that is, that there is no systematic bias due to inapplicability of the model; therefore, we have assumed that all uncertainties are either "statistical uncertainties", that is, coming from lack of knowledge about the parameters governing the models or "random uncertainties" due to simplifications. These assumptions do not strictly hold. For instance, we know that a bias is introduced due to the simple way used to consider the influence of lateral heterogeneities. However, knowledge of the stratigraphic profile contains some information that should not be kept out from the analysis. In computing response spectra with technique 2, we have not taken into account the possible dependence of empirical transfer functions on azimuth, and to fix the probability distributions of its ordinates we have used recordings of events originating at very different coastal locations. For summation of Green's functions we use an oversimplified rupture scheme; directivity effects, possible anomalous radiation -as observed during the Michoacán earthquake- and more complex and realistic rupture patterns are not accounted for, possibly

introducing a bias that is difficult to assess. Note, however, that although in technique 3 uncertainty comes only from variations in the time delays, we obtain a rather large variation from one simulation to another, as can be inferred from Fig. 11.

The procedure used to generate synthetic accelerograms in techniques 1 and 2 produces signals with time-invariant spectral shapes. This limitation is especially important when computing second statistical moments of inelastic spectral ordinates, since their coefficients of variation are usually underestimated. Note in Fig. 12 that the standard deviations of the logarithm of inelastic ordinates are of the same order of magnitude as those corresponding to elastic ordinates, while with techniques 1 and 2 the inelastic standard deviations are smaller than their elastic counterparts. This fact will be accounted for when combining estimates from the three techniques.

THE COMBINATION SCHEME

The estimations presented of response spectra are results of competing approaches. Each approach is correct to some extent, and since none includes all the information available, one would expect that a combination of the three is closer to the correct answer. We describe here a rational way to combine results, based on an earlier work [14].

The problem is similar to that of combining expert opinions. The expected response spectra obtained from each technique can be regarded as the answer of an expert to the question concerning response spectra at Station 56 from a postulated earthquake. As mentioned, we shall assume that answers from experts are unbiased and, furthermore, we shall assume that the computed second moments are measures of the uncertainty that each expert places on his estimation. On empirical bases several authors have adopted lognormal distributions for response spectral ordinates. We will also assign them a joint lognormal distribution, with median values and standard deviations computed as described previously, on the basis of χ^2 tests performed on earthquakes recorded on the Valley of Mexico which show that the assumption is tenable at the 0.05 level. Moreover, within bounds, the variance of a response spectral ordinate computed combining the three techniques is not very sensitive to the precise shape of the distributions (see Fig. 13) and the lognormal is intuitively appealing and mathematically tractable.

To fully define the joint distribution of the response spectral ordinates computed with the three techniques, we need also to assess the correlation scheme. To do this, we first computed the correlation coefficient between pairs of estimates directly from the simulations. We then smoothed the correlation functions (they are functions of the structural period) and modified them to account for the relatively small sample size and to introduce our own judgment about the coefficients of correlation. The uncertainty in the coefficients of correlation could have been formally dealt with using the Bayesian approach proposed in Ref. 14. However, the authors of that work conclude that results are much more sensitive to the relative values of the variances than to the correlation scheme. We also modified the variances of the inelastic spectral

ordinates computed with techniques 2 and 3 to take into account the problems caused by the lack of time evolution of the Fourier spectra when simulating ground motion. We assumed that the standard deviations of the logarithm of inelastic spectral ordinates were similar to those computed for elastic responses. In Figs. 14 and 15 we show the final standard deviations and correlation coefficients, respectively, used to fix the second-order moments of the joint distribution of estimates.

Let C be the matrix of covariances among the log-errors and x the vector of expected log-response spectral ordinates furnished by each technique or expert. If C is known -assigned- and no prior information is included, a formal Bayesian approach [14] leads to the conclusion that the combined estimate is also a lognormally distributed random variable with moments given by

$$\bar{x} = x^T C^{-1} j / h \quad (1)$$

$$h = j^T C^{-1} j \quad (2)$$

where \bar{x} and h are the mean and precision -the inverse of the variance-, respectively, of the log combined estimate, and j is a three-dimensional vector of ones. Note that Eqs. 1 and 2 imply that the mean value of the log-combined estimate is the weighted average of the opinions supplied by each technique. The weighting factors depend both on the relative precision of each technique and on the correlations between them.

Results of applying Eqs. 1 and 2 to the results obtained using the different strong-motion estimation techniques are shown in Fig. 16. Thus, for decision making purposes the response spectra due to the postulated earthquake should be regarded as a lognormally distributed random variable with the statistical moments given in this figure.

SUMMARY AND CONCLUSIONS

We estimated ground motion at a soft site of the Valley of Mexico in terms of elastic and inelastic response spectra for a hypothetical M 8.2 earthquake occurring in the Guerrero Gap, 280 km away from Mexico City. We used three different techniques which produce competing estimators of the quantities of interest, and we applied a combination scheme to end up with a single probability distribution of response spectral ordinates that includes all the information available.

Estimators from the different approaches are treated as lognormally distributed random variables; they are not independent since each technique makes use of information shared with the rest. Furthermore, each approach is associated with a different degree of precision, measured with the computed second-order moment. We included these facts in computing the probability distribution of the final estimator.

Results show, for instance, that given that a M 8.2 earthquake occurs at the postulated epicentral distance, the probability of the elastic response ordinate at 2.2 sec exceeding 1000 gals is about 50%, and that, for the same structural period, a pseudoacceleration of 1650 gals has a 1% probability of exceedance. It is also worth to note that the expected spectral ordinates for a ductility demand as low as 1.5 are 2.5 times lower than their elastic counterparts, showing the large reductions in acceleration due to inelastic behavior for narrow-band motions.

Several matters should be further looked into in order to improve on the present study. One is explicit consideration of statistical correlations between spectral ordinates for different periods and between those of linear behavior, those of nonlinear behavior and duration when using techniques 1 and 2. The procedure used to generate synthetic motions with these techniques does not allow for the inclusion of a prescribed correlation function. Another is use of evolutionary spectra which is particularly relevant to the elastoplastic responses, since an elastoplastic structure softens simultaneously with the general lengthening of ground motion periods.

In view of the existence of more than 100 accelerographic stations at the Valley of Mexico, the approach presented can be used to derive microzonation maps of Mexico City that combine, in a formal way, most of the knowledge that on ground motion at the city has been collected in the last years, with explicit probabilistic considerations and optimum design criteria.

ACKNOWLEDGEMENTS

Authors greatly appreciate suggestions made by S. K. Singh. This study was funded by Secretaría General de Obras (Departamento del Distrito Federal) and DGAPA (UNAM).

REFERENCES

1. Arciniega, A., "Modelo semiempírico para estimar espectros de respuesta sísmicos en el valle de México", thesis presented to the National Autonomous University of Mexico in partial fulfillment on the requirements for the degree of Geophysical Engineer, 1990.
2. Bard, P.-Y., M. Campillo, F.J. Chávez-García, and F.J. Sánchez-Sesma, "A theoretical investigation of large- and small-scale amplification effects in the Mexico City Valley", *Earthquake Spectra*, Vol. 4 (3), pp. 609-624, 1988.
3. Boore, D.M., "Stochastic simulation of high-frequency ground motions based on the seismological models of the radiated spectra", *Bulletin of the Seismological Society of America*, Vol. 73 (6), pp. 1865-1894, 1983.
4. Bravo, M.A., F.J. Sánchez-Sesma, and S. Chávez-Pérez, "A hybrid approach to study the seismic response of soft-soil sedimentary basins", in *Engineering Seismology and Site Response (Proceedings of the Fourth International Conference on Soil Dynamics and Earthquake Engineering)*, A.S. Cakmak and I. Herrera, editors, pp. 183-193, 1989.

5. Brune, J.N., "Tectonic stress and the spectra of seismic shear waves from earthquakes", *Journal of Geophysical Research*, Vol. 75, pp. 4997-5009, 1970.
6. Campillo, M., P.-Y. Bard, F. Nicollin, and F. Sánchez-Sesma, "The incident wave field in Mexico City during the great Michoacán earthquake and its interaction with the deep basin", *Earthquake Spectra*, Vol. 4 (3), pp. 591-608, 1988.
7. Joyner, W.B. and Boore, D.M., "On simulating large earthquakes by Green's function addition of smaller earthquakes", *Earthquake Source Mechanics*, Geophysical Monograph 37, Maurice Ewing Vol. 6. American Geophysical Union, pp. 269-274, 1986.
8. Ordaz, M., S.K. Singh, E. Reinoso, J. Lermo, J.M. Espinosa, and T. Domínguez, "Estimation of response spectra in the lake bed zone of the Valley of Mexico", *Earthquake Spectra*, Vol. 4 (4), pp. 815-834, 1988.
9. Ponce, L., L. Granados, D. Comte, and M. Pardo, "Seismicity and Q-coda temporal variation in the Guerrero, Mexico, seismic gap: evidences for a soon-to-break gap?" (Abstract), *Seismological Research Letters*, Vol. 61 (1), pp. 43, 1990.
10. Ponce, L., M. Pardo, D. Comte, and G. Malavé, "Spatio-temporal analysis of the Guerrero, Mexico, seismic gap seismicity ($m_b = 4.5$): a quiescent subregion lasting 14 years", *Bulletin of the Seismological Society of America*, submitted.
11. Rosenblueth, E. and M. Ordaz, "Maximum earthquake magnitude at a fault", *Journal of Engineering Mechanics (ASCE)*, Vol. 116 (1), pp. 204-216, 1990.
12. Sánchez-Sesma, F.J., S. Chávez-Pérez, M. Suárez, M.A. Bravo, and L.E. Pérez-Rocha, "On the seismic response of the Valley of Mexico", *Earthquake Spectra*, Vol. 4 (3), pp. 569-589, 1988.
13. Seed, H.B., M.P. Romo, J.I. Sun, A. Jaime, and J. Lysmer, "Relationships between soil conditions and earthquake ground motions", *Earthquake Spectra*, Vol. 4 (4), pp. 687-729, 1988.
14. Stauffer, D., "Programming cellular automata", *Computers in Physics*, Jan/Feb, pp. 62-67, 1991.

TABLE 1. EARTHQUAKES RECORDED IN MEXICO CITY SINCE 1985

DATE (y.m.d)	ORIGIN a	M	R (km)	NUMBER OF DATA				
				b	c	d	e	f
85.09.19	SM	8.1	380	11	-	-	11	1150
85.09.21	SM	7.6	320	7	-	-	7	680
86.04.30	SM	7.0	410	7	-	-	7	400
87.03.12	L	3.0	-	1	2	-	3	45
87.06.07	SG	4.8	270	6	7	-	13	480
87.07.15	NO	5.9	280	10	7	-	17	1020
88.02.08	SG	5.8	290	55	5	-	60	3910
89.03.10	SG	5.0	240	13	-	-	13	330
89.04.25	SG	6.9	305	66	2	-	68	12430
89.05.02	SG	5.0	305	50	3	-	53	3280
89.08.12	?	5.5	220	14	3	-	17	370
90.05.11	SG	5.3	295	51	4	5	60	3930
90.05.31	SG	6.1	295	71	7	16	95	8800

Notes:

a) S=subduction zone event; L=local event; N=normal fault event; M=State of Michoacán; G=State of Guerrero; O=State of Oaxaca.

b) Free-field accelerographs that recorded the event.

c) Building accelerographs that recorded the event.

d) Bore-hole accelerographs that recorded the event.

e) Total number of accelerographs that recorded the event.

f) Total recording time produced by the earthquake, in sec.

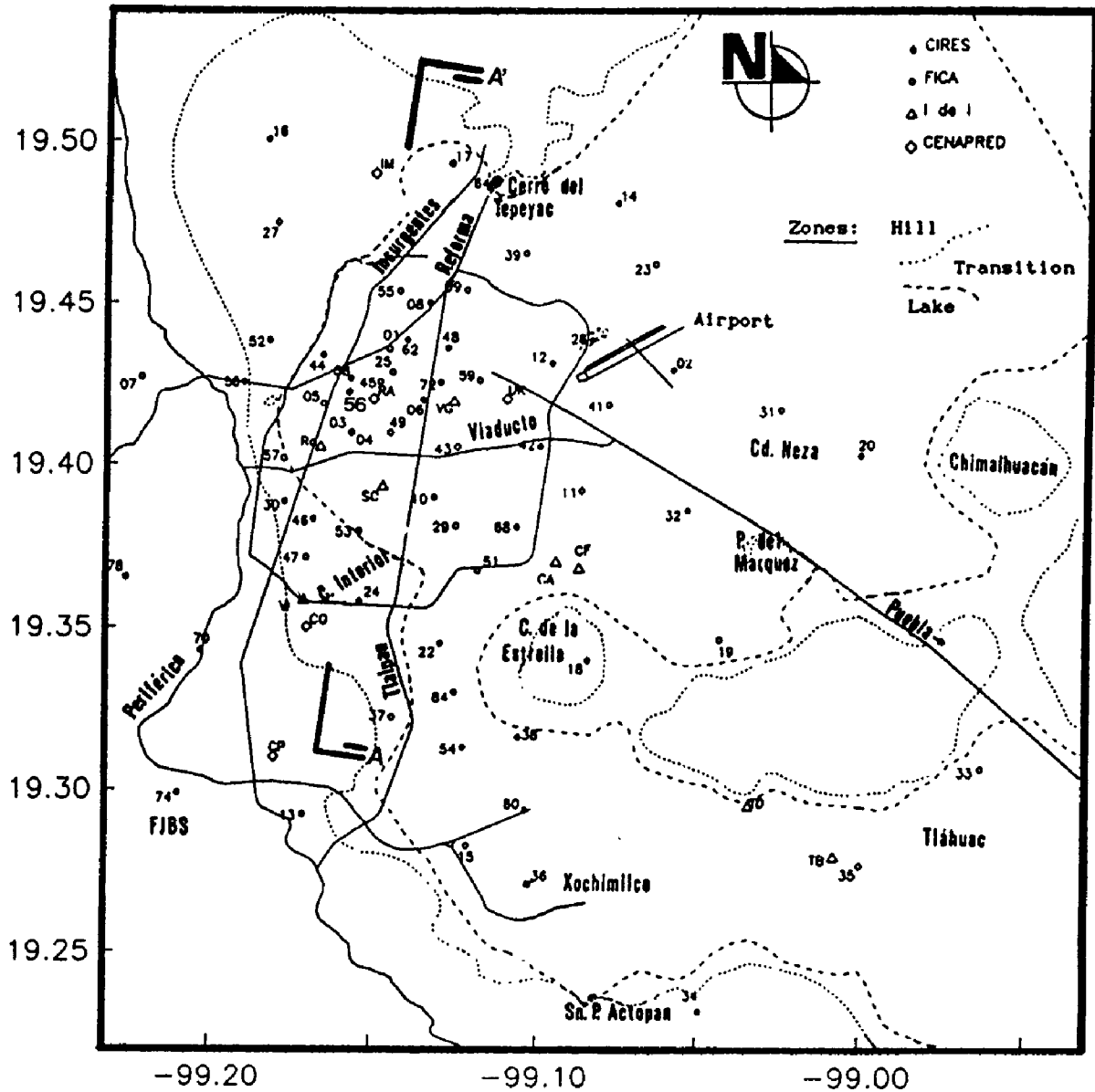


Fig. 1 Map of Mexico City showing locations of strong-motion instruments, operated by different institutions (see top right corner). Dotted line denotes the border between hill and transition zones, while dotted line shows the border between transition and lake-bed zones. Solid lines are the main avenues. Note Station 56, approximately at 19.42°N and 99.16°W.

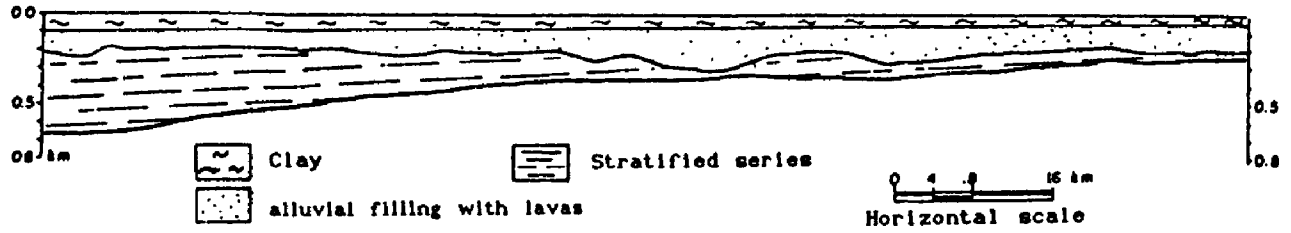


Fig. 2 Section A-A' (see Fig. 1), roughly NS across the most densely populated area of Mexico City.

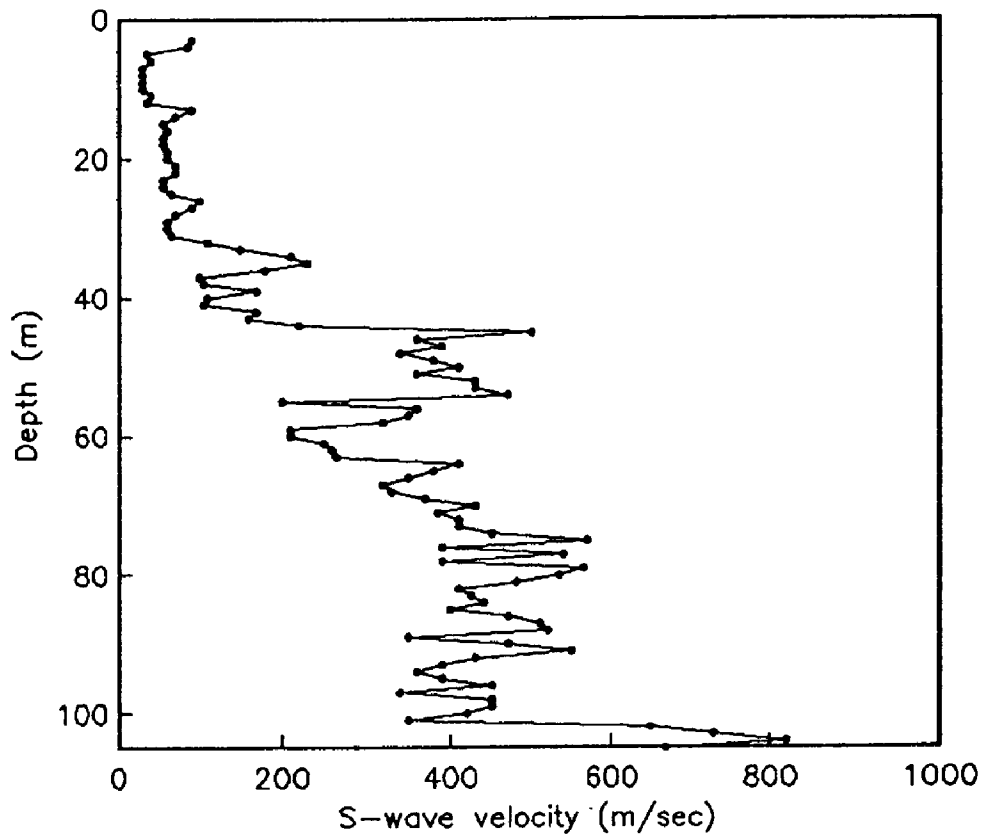


Fig. 3 S-wave velocity profile at a soft site of the Valley of Mexico.

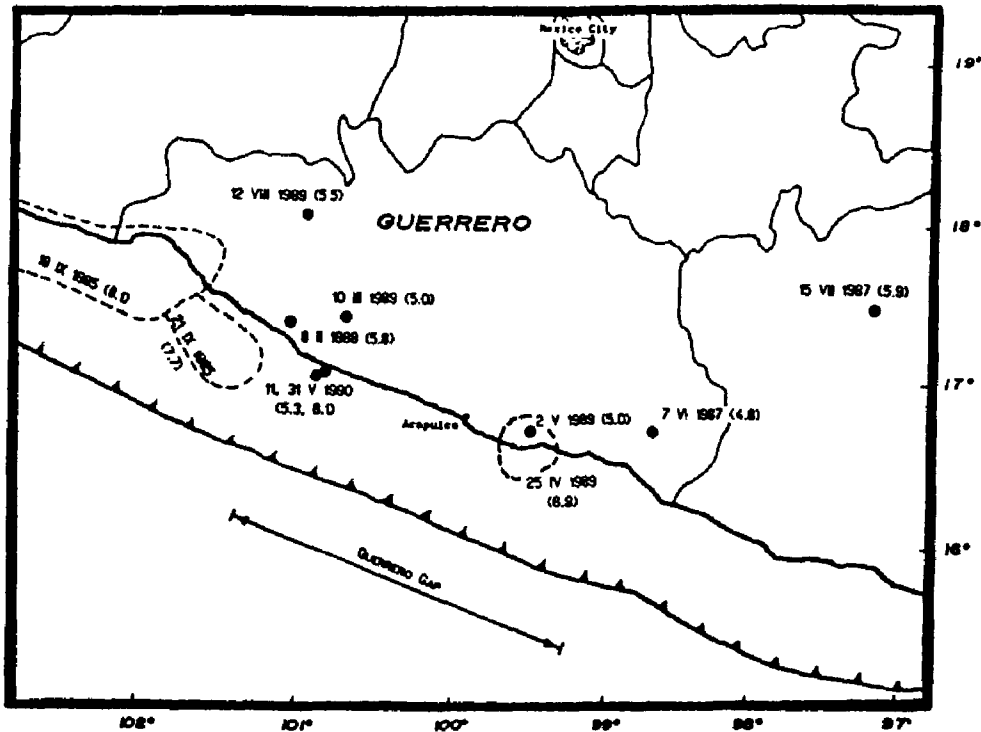


Fig. 4 Partial map of the Pacific coast of Mexico showing epicenters of earthquakes (solid dots) whose strong motions were recorded at Mexico City. Dashed lines show the rupture areas of the largest three events. Numbers between brackets are magnitudes.

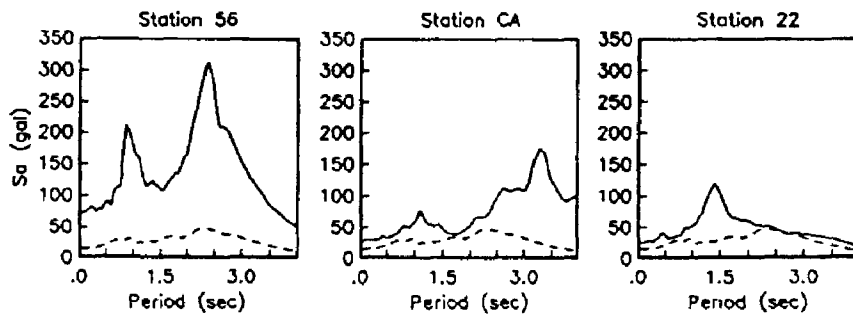


Fig. 5 Sample of response spectra (pseudoaccelerations, 5% of critical damping) computed from recordings of the April 25, 1989 ($M=6.9$) earthquake at different sites of the Valley of Mexico. The spectrum obtained from the CU recording (a hill-zone site) is shown with dotted line for reference. The title in each box indicates the number or code of the station (see Fig. 1 for locations).

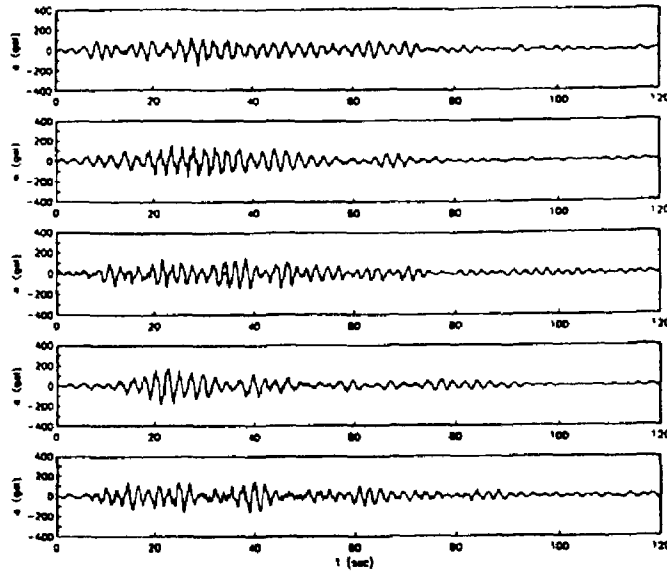


Fig. 6 Sample of synthetic accelerograms generated with technique 1 for Station 56 ($M=8.2$, $R=280$ km).

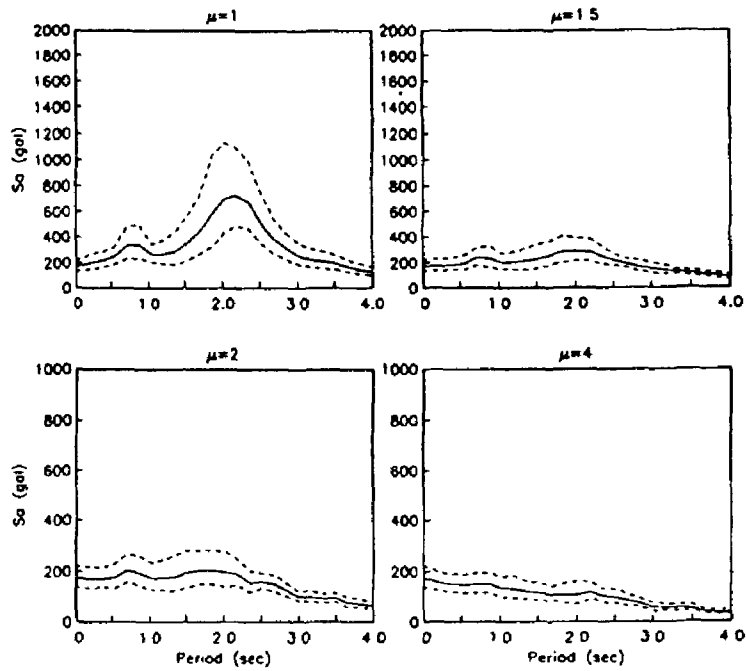


Fig. 7 Response spectra associated with percentiles 50 (solid line), 16 (upper dotted line) and 84 (lower dotted line) computed with technique 1, for several ductility demands, μ .

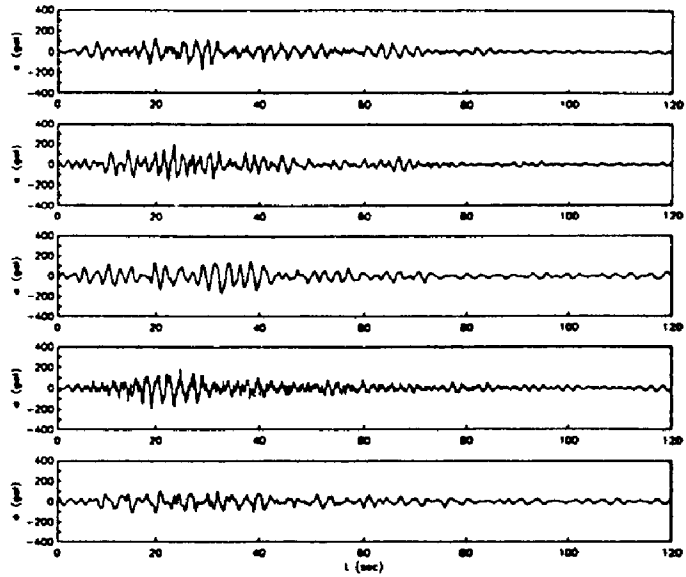


Fig. 8 Sample of synthetic accelerograms generated with technique 2 for Station 56 ($M=8.2$, $R=280$ km).

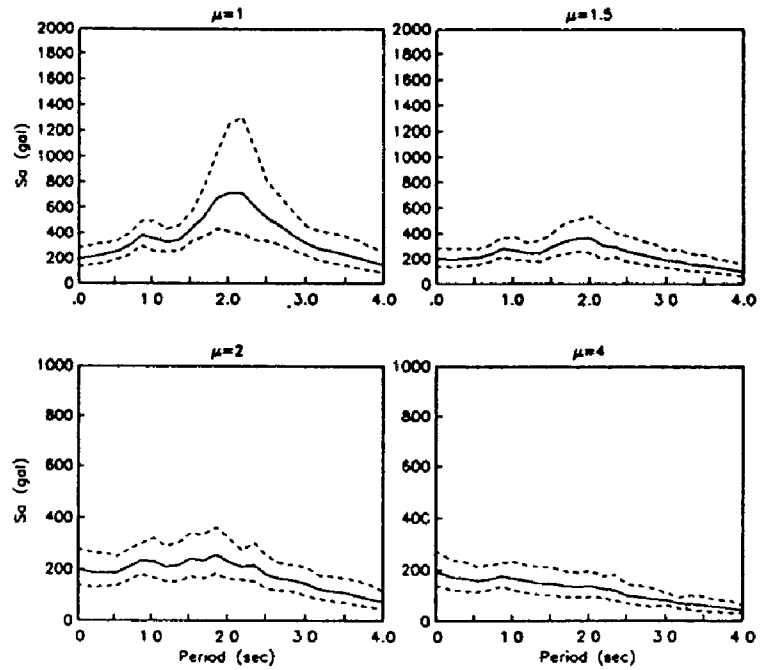


Fig. 9 Response spectra associated with percentiles 50 (solid line), 16 (upper dotted line) and 84 (lower dotted line) computed with technique 2, for several ductility demands, μ .

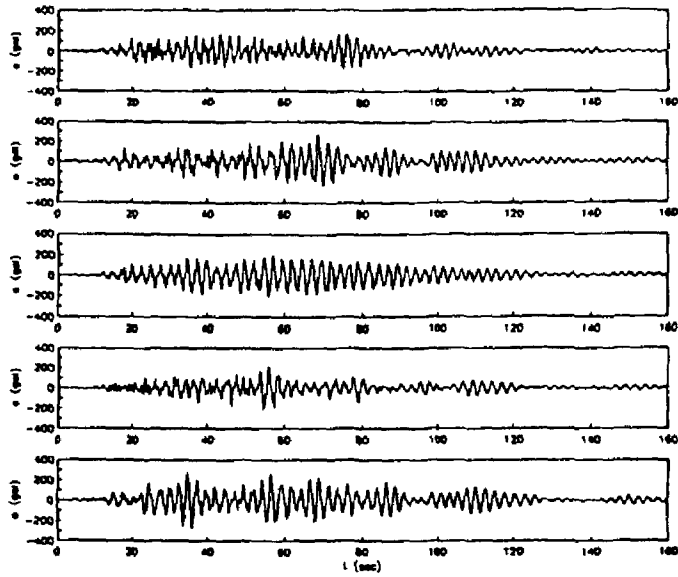


Fig. 10 Sample of synthetic accelerograms generated with technique 3 for Station 56 ($M=8.2$, $R=280$ km).

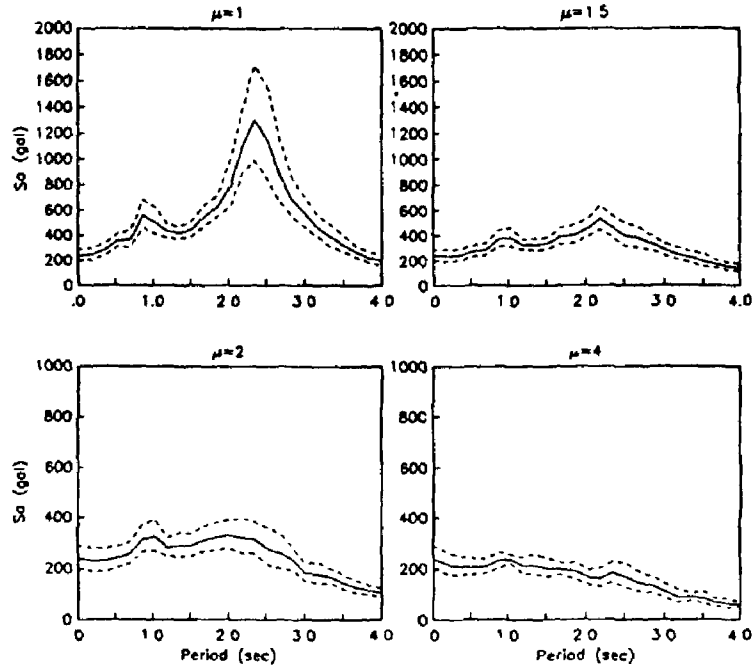


Fig. 11 Response spectra associated with percentiles 50 (solid line), 16 (upper dotted line) and 84 (lower dotted line) computed with technique 3, for several ductility demands, μ .

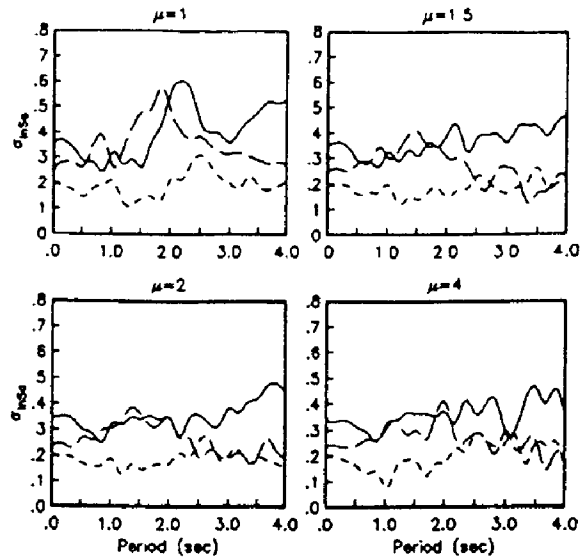


Fig. 12 Standard deviations of the natural logarithm of response spectral ordinates, $\sigma_{\ln S_a}$ for several ductility demands, μ , obtained by simulation with the three techniques. Dashed line: technique 1; solid line: technique 2; dotted line: technique 3.

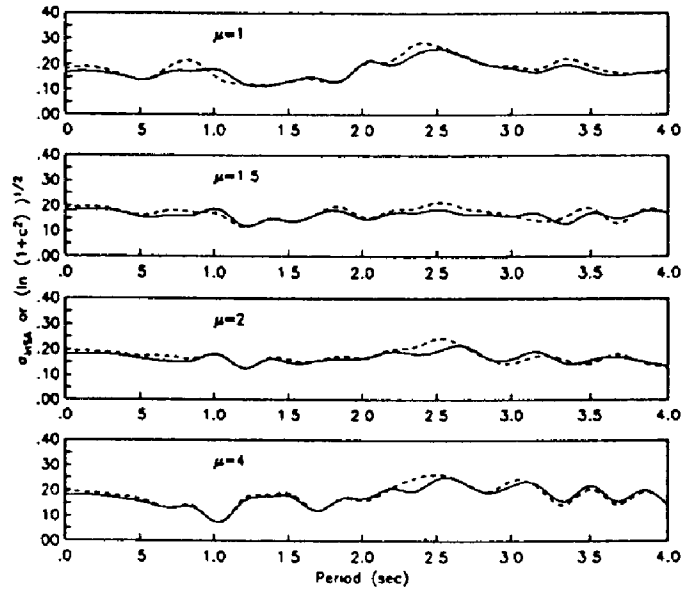


Fig. 13. Final second moments of response spectral ordinates, for several ductility demands, μ , computed assuming two different distributions for predicted responses from each technique. Solid line: standard deviation of the natural logarithm of responses, $\sigma_{\ln S_a}$, assuming lognormal distribution; dotted line: $[\ln(1+c^2)]^{1/2}$, where c is the coefficient of variation, assuming normal distribution.

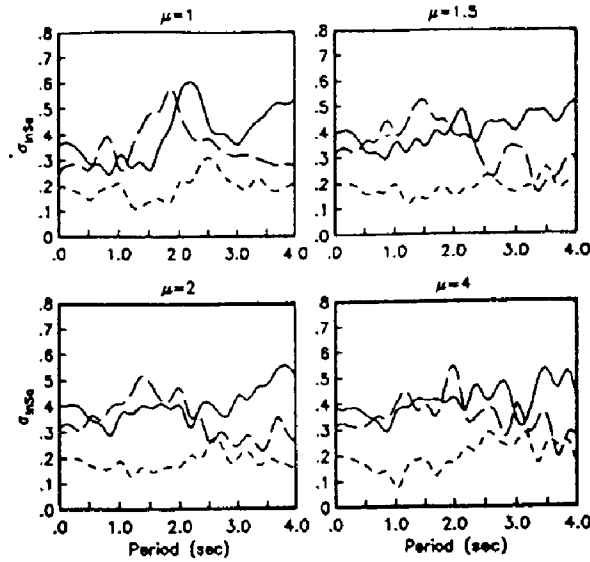


Fig. 14 Standard deviations of the natural logarithm of response spectral ordinates, $\sigma_{\ln S_a}$, for several ductility demands, μ , obtained modifying those shown in Fig. 12 as described in the text. Dashed line: technique 1; solid line: technique 2; dotted line: technique 3. These values, in conjunction with the coefficients of correlation of Fig. 14 were used to form the final matrix of covariances to apply the combination scheme.

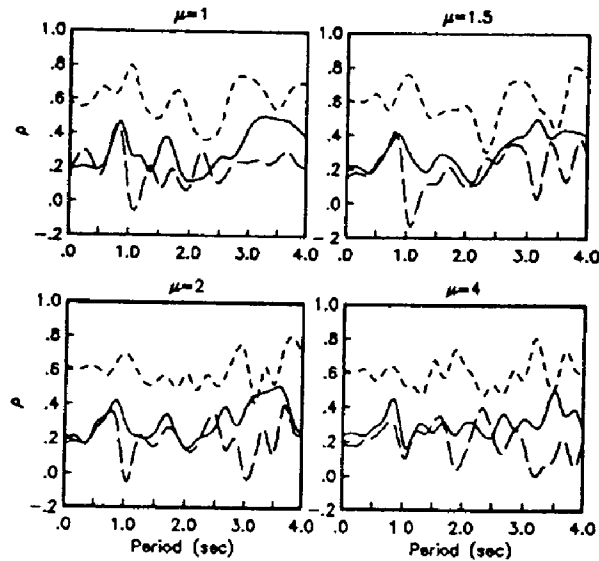


Fig. 15 Coefficients of correlation of the natural logarithm of response spectral ordinates, ρ , for several ductility demands, μ , obtained with the three techniques. Dotted line: coefficient of correlation between techniques 1 and 2; dashed line: between techniques 1 and 3; solid line: between techniques 2 and 3. These values, in conjunction with the standard deviations of Fig. 14 were used to form the final matrix of covariances to apply the combination scheme.

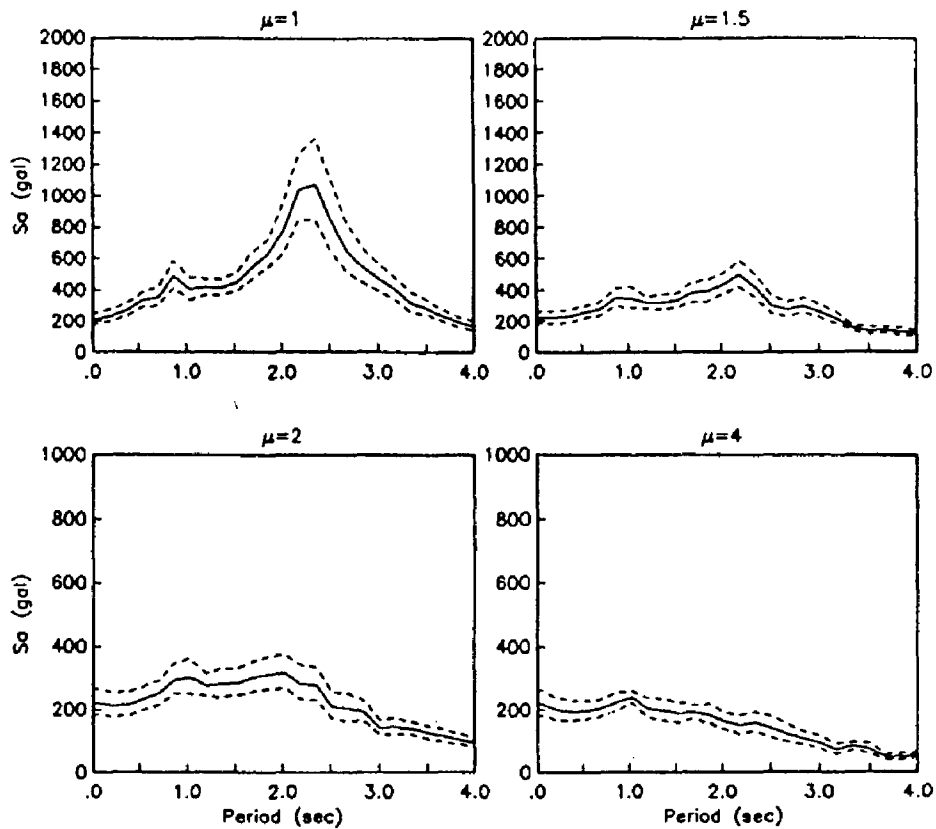


Fig 16. Final response spectra associated with percentiles 50 (solid line), 16 (lower dotted line) and 84 (upper dotted line), for several ductility demands, μ , obtained combining estimates from the three techniques.